J. Comp. App. Res. Mech. Eng. Vol. 15. No. 2, pp. 233-250, 2026 *DOI: 10.22061/jcarme.2026.113064.2825*

Journal of Computational and Applied Research in Mechanical Engineering

jcarme.sru.ac.ir

SRTTU

JCARME

ISSN: 2228-7922

Research paper

The estimation of the fatigue life of an intact gas turbine compressor blade and the same blade with foreign object damage based on critical plane methods

A. R. Shahani[*] and A. Zolfaghari

Department of Applied Mechanics, Faculty of Mechanical Engineering, K.N. Toosi University of Technology, Tehran, Tehran, 19395-1999, Iran

Article info:

Article history:

Received: 13/005/2026

Revised: 05/08/2026

Accepted: 08/08/2026

Online: 11/08/2026

Keywords:

Fatigue life prediction,

Gas turbine compressor,

Foreign object damage (FOD),

Critical plane method,

Structural integrity.

[*]Corresponding author: *shahani@kntu.ac.ir*

Abstract

The first-stage compressor blades of the gas turbine are subject to occasional failure due to their operating conditions. Initial evaluations indicate that microcracks forming in critical areas of the blade under fatigue loading make the blade prone to failure. Therefore, it is of great importance to find the locations of the blade where microcracks are most likely to form. In this study, extensive numerical and analytical investigations were conducted to evaluate the observed failures, and Abaqus software was used for finite element analysis of the first-stage compressor blade of the gas turbine model. In pursuit of this goal, initially, finite element simulations were conducted on an intact blade, followed by analyses on a blade incorporating a V-shaped notch, and subsequently, applying stress analysis, the critical positions that are the main candidates for the formation and initiation of microcracks in the blade were determined. In addition, a new critical plane fatigue model was applied to evaluate and investigate the fatigue behaviour of the compressor blade. Then, through coding in MATLAB software, the plane that suffered the maximum damage based on the critical plane fatigue model was determined, and its direction was calculated for the critical positions of the compressor blade. Finally, the compressor blade fatigue life was determined based on this criterion and compared with traditional critical plane fatigue criteria such as Brown-Miller and SWT, and the reduction in life due to foreign object damage to the blade was determined and compared to an intact blade.

1. Introduction

A gas turbine represents a category of internal combustion engines, comprising an upstream rotating compressor mechanically coupled to a downstream turbine, and there is also a combustion chamber between them. Axial compressors serve as pivotal components within gas turbine engines, performing the essential function of compressing the air

subsequently introduced into the combustion system.

Compressor discs and blades typically function under low-temperature conditions while experiencing high rotational velocity, thereby subjecting the blades to substantial centrifugal loads; therefore, during engine start-up and shutdown, the first component suffering major fatigue damage (Fig. 1) is the compressor blades [1].

Compressor blades are frequently prone to failure due to the initiation and subsequent propagation of fatigue-induced cracks. The initiation of cracks in compressor blades is governed by surface imperfections such as nonmetallic inclusions, corrosion pits, and dents [2]. Previously, Kermanpour [3], Siluria [4], and Paznaska [5] have reported problems with compressor blades.

Numerous reports of problems with first-stage compressor blades in gas turbines, such as those in Pakistan, China, Korea, and the United States, as well as Iran, indicate similar failures due to design errors.

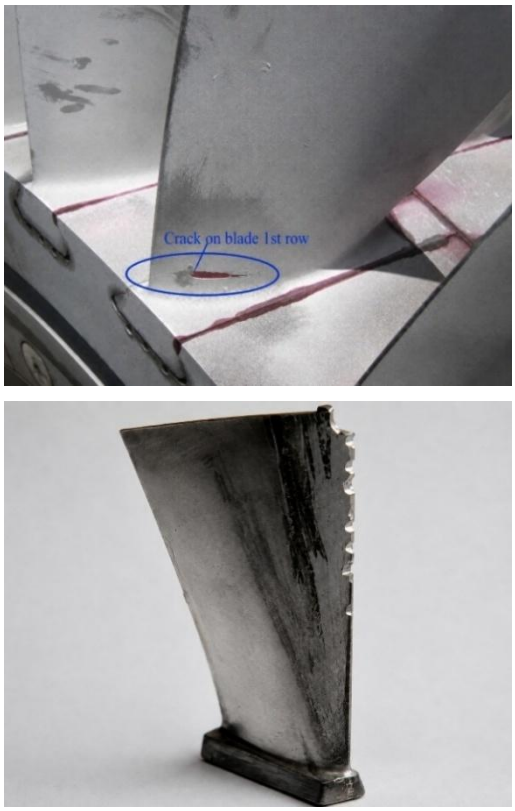


Fig. 1. Cracked blade detected (upper figure) and blade with defect due to foreign object damage (lower figure) during repair assessment.

Consequently, premature and unforeseen fracture of a blade, accompanied by the impact of the detached segment on adjacent blades, can precipitate the failure of the entire compressor assembly.

Regarding the critical significance of this phenomenon, several specialized conferences have been convened to investigate these challenges, and there have been cases of premature failure of compressor blades in four gas turbines at coastal refineries, including failures after approximately 26,780 operating hours for the GTG-A turbine in September 2006, 31,599 operating hours for the GTG-B turbine in October 2006, 30,895 operating hours for the GTG-D turbine in March 2008, and 18,000 operating hours for the GTG-C turbine in October 2010, and all failures have occurred in the first stage of the moving blades [6].

To some extent, compressor blades determine the life and safety of the entire engine. These compressor blades are susceptible to fatigue-induced damage resulting from cyclic loading, and such deterioration is notably more pronounced during engine start-up and shutdown phases compared to steady-state operation.

Factors including material characteristics, manufacturing techniques, operation under harsh environments, and complex loading scenarios [7-10] exacerbate the fatigue failure mechanisms of compressor blades and substantially complicate the accurate prediction of their service life.

The failure of axial compressor blades is often associated with localized stress concentration regions caused by geometric discontinuities, assembly conditions, and complex operational loading. Previous studies have shown that blade root regions are highly susceptible to crack initiation due to the combined effects of centrifugal forces, aerodynamic loads, and blade–disk contact interactions [11].

Finite element investigations have also demonstrated that small geometric features and contact conditions can significantly modify stress distribution and accelerate damage accumulation in rotating blades. Therefore, accurate evaluation of critical stress concentration zones is essential for reliable fatigue life assessment of compressor blades.

As a consequence, the challenge of reliably predicting blade fatigue life remains unresolved, leading to considerable repair and maintenance expenditures and undermining the operational reliability of gas turbine systems.

In addition, fatigue damage is considered one of the most important factors limiting the service life of gas turbine components; therefore, various fatigue mechanisms and life prediction approaches have been investigated for compressor blades subjected to complex service-induced mechanical loading conditions. Such approaches provide a better understanding of fatigue behavior and enable more reliable life estimation by accounting for the combined effects of multiaxial loading, stress concentration, and other operational factors influencing the structural integrity of critical blade regions.

Fatigue life prediction techniques can be categorized into four principal approaches: the critical plane method, the energy-based method, the equivalent stress method, and the equivalent strain method. Fatigue life prediction approaches mainly comprise equivalent strain-based models, energy-based criteria, and critical plane methodologies. Within this framework, the equivalent strain method for multiaxial loading employs an equivalent uniaxial loading and, by combining it with the uniaxial Coffin–Manson equation, predicts the fatigue life.

Yokobori *et al.* [12] first introduced the equivalent strain theory. This theory included the maximum shear strain model, the maximum principal strain model, and the von Mises equivalent strain model. This approach does not establish a definitive physical correlation between the equivalent strain and fatigue life, and it overlooks the coupled influences of stress–strain interactions and loading parameters.

Morrow [13] proposed the energy method, and Ostergren [14] first applied it to predict uniaxial fatigue life; then Garud [15] and Ellyin [16] proposed a multiaxial fatigue prediction model and plastic strain energy, and Lee *et al.* [17] applied the summation of elastic and plastic strain energies as a fatigue damage parameter.

Brown and Miller [18, 19] assume that crack initiation and propagation occur on a plane with maximum shear strain as the damage parameter, and as a result, they consider the maximum shear strain and normal strain on that plane; the Kandile-Brown-Miller model [20] considers the maximum shear strain range and normal strain range as the damage parameter.

Fatemi and Socie [21] considered a model based on the Kandile-Brown-Miller model, in which the maximum shear strain range and normal stress on a critical plane were applied, and its damage parameter is the maximum shear strain range. The SWT model [22], by combining the Smith, Watson, and Topper models, considers the maximum normal strain range and the maximum normal stress on a plane with maximum normal strain.

Despite the development of numerous fatigue life prediction models, the inherent complexity of fatigue phenomena has so far precluded the establishment of a universally applicable model. In recent years, many researchers, such as Shang De-Guang [23] and Yu Zheng-yong [24], have conducted comprehensive revisions and enhancements to critical plane models and derived new multiaxial fatigue life prediction models.

The applicability of critical-plane-based fatigue approaches has also been demonstrated in realistic turbine operating conditions. Lu *et al.* [25] applied a critical-plane-based methodology to investigate the creep–fatigue damage behavior of single-crystal turbine blade tenons subjected to high-speed rotational loading and elevated temperatures.

Their experimental and numerical results revealed that the critical damage location was successfully identified in regions experiencing severe stress concentration, and the predicted fatigue life showed good agreement with experimental observations. This study confirms the capability of critical plane approaches in capturing the complex multiaxial stress-strain interactions governing crack initiation and life degradation in advanced turbine components under service-like conditions.

Also, researchers have investigated the creep-fatigue damage mechanism and life prediction in various materials and structures. Xiao *et al.* [26] conducted low-cycle creep-fatigue tests on FGH96 superalloy used in turbine disks at

550°C under different load-holding times and studied the fracture mode.

Wang *et al.* [27] investigated the creep–fatigue damage mechanism of a nickel-based single-crystal material under stress-controlled conditions at various temperatures and load-holding durations. Hu *et al.* [28] evaluated the creep-fatigue crack propagation under different load-holding times at 980°C, and Zhang *et al.* [29] established a damage-mechanics-based creep–fatigue reliability model using failure load data.

Shahani *et al.* [30] evaluated the creep-fatigue phenomenon in a high-pressure gas turbine blade, considering both the presence and absence of creep-fatigue interaction. Experimental determination of the gas turbine blade's lifetime was conducted using specimens that replicated the blade's physical conditions, and the numerical results of the study were validated accordingly.

The results demonstrate that disregarding the creep–fatigue interaction can introduce substantial inaccuracies in predicting the service life of gas turbine blades.

Compressor blades are susceptible to foreign object damage, and the ingestion of foreign objects into the core of a gas turbine engine can induce significant structural damage to compressor blades. The intense airflow necessary for engine operation generates a strong suction, capable of entraining small objects from the surrounding environment.

Compressor blade damage is usually caused by particles striking the rotating blades, and it often takes the form of dents or notches at or near the leading edge of the compressor (Fig. 2). Damage from hard particles with millimeter-scale dimensions during compressor operation can lead to unexpected fatigue failure [31].

Li *et al.* [32] developed a three-dimensional crack growth framework to investigate the influence of vibratory loading on fatigue crack propagation in compressor blades subjected to high-cycle fatigue conditions. Their study indicated that variations in loading conditions and crack characteristics can significantly affect crack growth behavior and fatigue life estimation.

These observations highlight the importance of considering the interaction between local damage features, loading conditions, and fracture-related parameters for reliable fatigue assessment of compressor blades.

Yin *et al.* [33] proposed a modified mean stress-based model to predict the high-cycle fatigue strength of Ti-6Al-4V compressor blades subjected to foreign object damage (FOD).

The investigation revealed that conventional fatigue notch correction approaches, such as Peterson and Neuber models, exhibit considerable prediction deviations when applied to FOD-induced damage, particularly under oblique impact conditions. The results indicated that the impact angle and tensile residual stresses generated during the damage process significantly influence the fatigue strength reduction of damaged specimens.

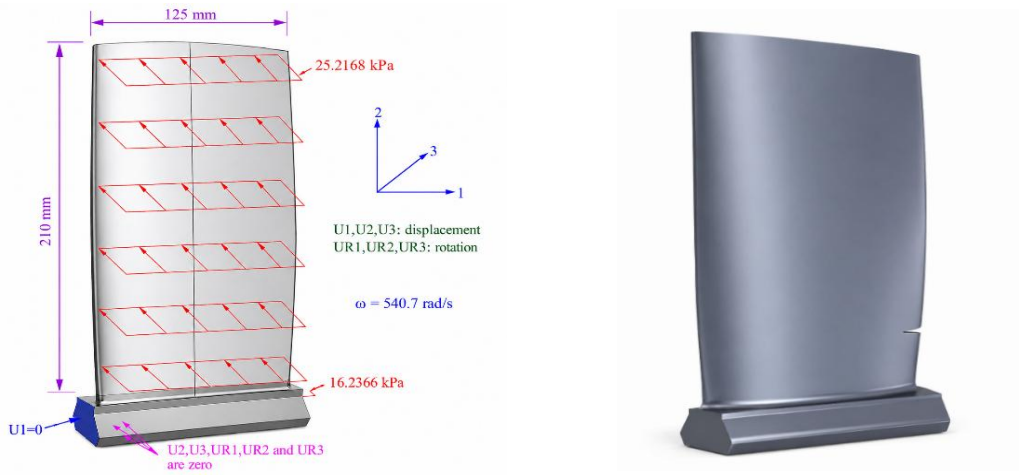


Fig. 2. Loads and boundary conditions on an intact blade (left figure) and a picture of a blade with damage caused by a foreign object (V-shaped notch in the right figure).

By incorporating a shear correction factor and residual stress effects into the prediction framework, the proposed approach achieved improved agreement with experimental results compared with conventional models.

Moradi *et al.* [34] investigated the crack growth behavior of compressor blades subjected to foreign object damage (FOD) and resonant vibration conditions using a finite element-based approach. In their work, the stress distribution around the damaged region was evaluated, and the crack propagation process was simulated based on stress intensity factor calculations and fatigue crack growth modeling. The results showed that FOD-induced defects act as critical stress concentration sites and significantly accelerate crack propagation, particularly under resonant vibration conditions.

Their findings demonstrated that the combined effects of damage geometry and dynamic loading conditions play a crucial role in reducing the fatigue life of compressor blades.

Although numerous studies have investigated fatigue life prediction of gas turbine compressor blades, limited attention has been given to the comparative assessment of fatigue damage evolution between intact and foreign-object-damaged blades using different critical plane criteria.

Moreover, the influence of selecting different multiaxial fatigue damage parameters on the predicted life reduction caused by FOD remains insufficiently explored. Therefore, the main contribution of this study is not the development of a new fatigue criterion, but the systematic evaluation of existing critical plane approaches, including the Shang De-Guang, Brown–Miller, and Smith–Watson–Topper criteria, for damaged and undamaged compressor blades under realistic multiaxial loading conditions.

The proposed methodology provides insight into the sensitivity of fatigue life predictions to the selected damage parameter and clarifies the role of FOD-induced stress concentration in fatigue degradation.

In this study, a compressor blade from a gas turbine engine that is completely intact and a defective blade similar to the intact blade were selected; then a V-shaped notch with a radius of 0.02 mm and a length of 3 mm was modeled on the compressor blade to simulate foreign object damage.

The dimensions of the V-shaped notch were selected to represent a realistic surface discontinuity associated with foreign object damage. The selected geometry provides a representative stress concentration condition while avoiding excessive localization caused by an unrealistically severe defect. The notch geometry has a significant influence on fatigue behavior, as variations in notch length and root radius directly affect local stress concentration and strain accumulation. Generally, deeper and sharper notches increase stress concentration, accelerate crack initiation, and reduce fatigue life, whereas smoother geometries with larger root radius led to improved fatigue resistance.

Through numerical evaluations, experimental observations, and stress analysis, the critical areas in both compressor blades were determined, and then fatigue in the blades was investigated based on multiaxial fatigue and critical plane criteria. Initially, by examining and determining the critical parameters of each selected criterion (Smith–Watson–Topper, Brown–Miller, and Shang De-Guang), the orientations of the critical planes, which indicate the region of crack initiation and propagation, were determined.

Subsequently, the fatigue life of the compressor blades was evaluated based on various critical plane criteria, and the assessment results for the intact blade and the blade with foreign object damage were compared with each other. Finally, it was shown that under the blade's operating conditions, the fatigue life of the blade with foreign object damage is significantly reduced and limited compared to that of the intact blade; this is while the intact blade theoretically has an infinite life based on the safe-life design approach.

The intact blade shows infinite fatigue life under the applied loading conditions. Here, the term "infinite fatigue life" refers to the conventional fatigue classification in which the predicted life exceeds 10^6 cycles and the applied stress level remains below the material endurance limit. However, this definition represents the theoretical fatigue behavior under the assumed loading conditions and does not imply an unlimited service life for practical components.

2. Finite element stress analysis

In this study, the compressor blades were modeled and fabricated in SolidWorks software, and the material used in the compressor blade was AISI Custom 450 stainless steel; its

mechanical, fatigue, and chemical analysis properties are given in Tables 1-3 [35].
In Table 1, ρ represents the material density, E is Young's modulus, σ_y and σ_u denote the yield strength and ultimate tensile strength, respectively, and υ represents Poisson's ratio. In Table 2, σ_f' and ε_f' are the fatigue strength and fatigue ductility coefficients, respectively; b and c represent the fatigue strength and fatigue ductility exponents, while K' and n' denote the cyclic strength coefficient and cyclic strain hardening exponent, respectively.
To mitigate the risk of catastrophic failures of compressor blades, which can ultimately result in the destruction of a gas turbine, a finite element analysis of the compressor blade was conducted using Abaqus software, and for this analysis, cubic elements of the second order (C3D20R) were applied.
The blade connection at its root section is a rigid one; therefore, for applying the boundary conditions, the displacements and rotations of the blade root were completely constrained. The pressure on the blade, caused by the air entering the compressor, causes bending and twisting, and the blade acts like a cantilever beam. There are two methods in Abaqus software to simulate aerodynamic loads: 1- applying pressure on the concave (compressive) side of the blade and 2- applying tangential force, axial force, and torsional moment on the blade.
In this simulation, a compressive load was applied to the compressor blade, and three methods can be used to study the aerodynamic load applied to the blade: experimental models, turbomachinery theory, and computational fluid dynamics (CFD). Computational fluid dynamics analysis has been previously performed using the commercial Fluent package [6 and 36].
Computational fluid dynamics results indicate that the axial and tangential loads vary linearly with the blade length, such that the magnitude of these forces is minimum at the blade hub and reaches its maximum at the blade tip.
Consequently, the pressure distribution resulting from the tangential and axial forces is trapezoidal and is applied to the pressure (concave) side of the blade. The pressure magnitude at the hub and blade tip is 16.2366 kPa and 25.2168 kPa, respectively. Also, the nominal angular velocity of the compressor blade is 540.7 rad/s (5163 rpm) [37]. Fig. 2 shows the boundary conditions and loading applied in Abaqus software as well as the defective blade (V-shaped notch).
The mesh shapes of intact and defective blades caused by foreign object damage (V-shaped notch) are shown in Fig. 3. Initially, the stress distribution due to centrifugal loading was determined by considering the boundary conditions and the angular velocity of the compressor blade.
According to Fig. 4, in the intact blade, the maximum von Mises stress (489.2 MPa) due to centrifugal loading is located in the fillet region of the convex (suction) side of the blade, and the maximum von Mises stress (626.6 MPa) in the blade with a V-shaped notch is located in the notch region, and fully fixed boundary conditions were applied at the blade root to evaluate the stress distribution induced by aerodynamic loading.
Also, a trapezoidal pressure distribution of 25.2161 kPa at the blade tip and 16.2366 kPa at the blade hub was applied on its pressure side. The results of the stress analysis due to aerodynamic loading indicate that the critical region is located on the pressure side of the intact blade and in the blade with a V-shaped notch; it is located in the blade notch (Fig. 5).

Table 1. Mechanical properties of AISI custom 450.

ρ (kg/m^3)	Hardness (Rockwell C)	E (GPa)	σ_y (MPa)	σ_u (MPa)	υ
7750	28	200	814	986	0.29

Table 2. Fatigue properties of AISI custom 450.

σ_f' (MPa)	b	ε_f'	c	K' (MPa)	n'	Fatigue strength (MPa)
2317	-0.084	0.25	-0.7	1743	0.059	517

Table 3. Chemical analysis of AISI custom 450.

C	Si	Mn	P	S	Cr	Ni	Mo	Cu
0.02	0.46	0.37	0.021	0.004	14.8	6.47	0.77	1.5

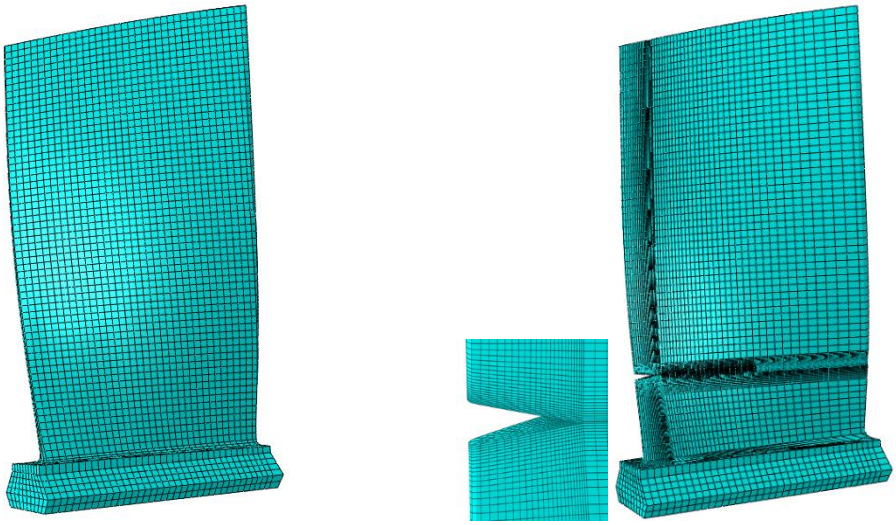


Fig. 3. Shapes of an intact blade mesh and a blade with a V-shaped notch.

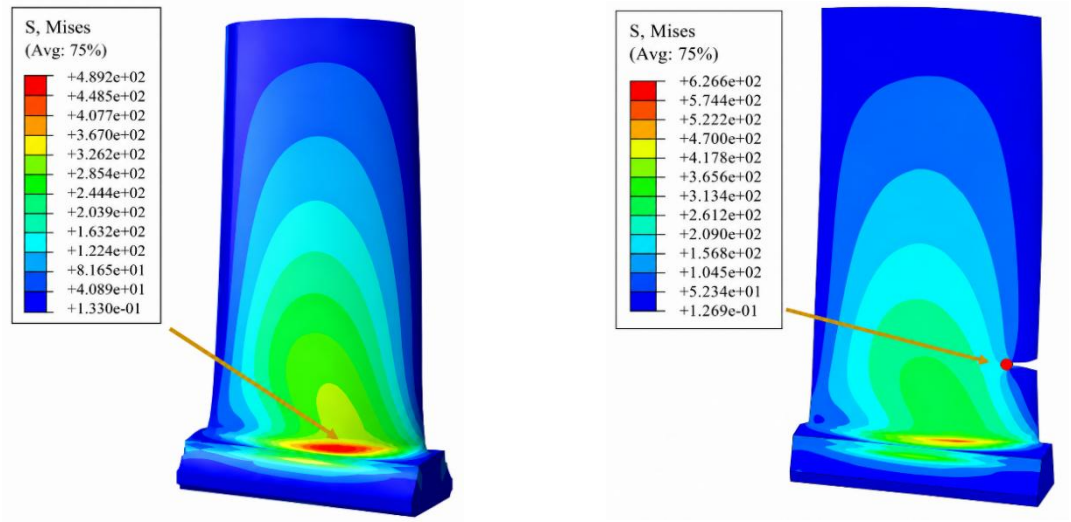


Fig. 4. Von Mises stress distribution in intact blades with a V-shaped notch compressor ones under centrifugal loads.

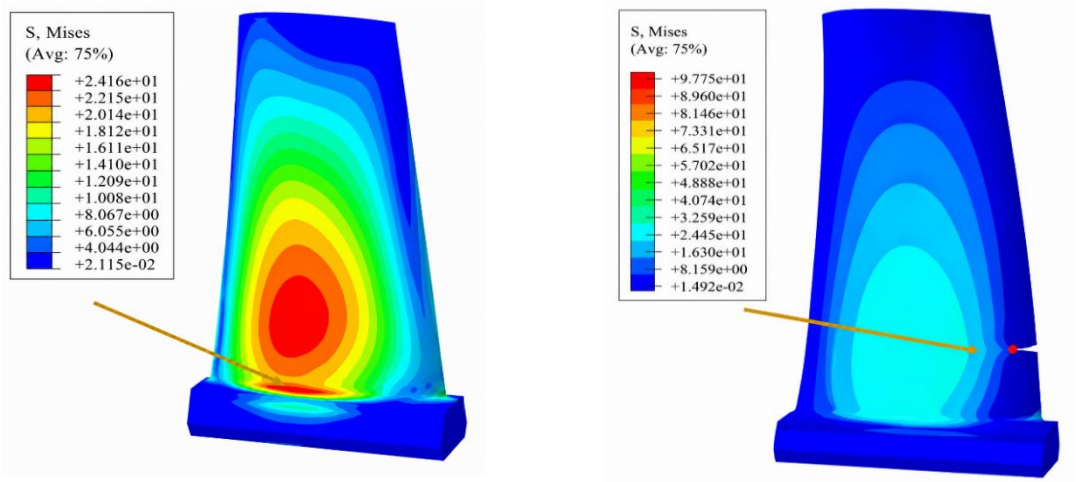


Fig. 5. Von Mises stress distribution in intact and V-shaped notch compressor blades under aerodynamic loads.

To investigate the combined effect of centrifugal and aerodynamic loads, a separate stress analysis was performed. In these analyses, aerodynamic loads, which are the cause of high-cycle fatigue, are superimposed on centrifugal loads, which are the cause of low-cycle fatigue. The stress ratio for centrifugal load was R=0 and for aerodynamic load was R=0.83.

The areas of maximum stress during this loading were named point A for the intact blade and point B for the blade with a V-shaped notch. The stress distribution contour of the combined centrifugal and aerodynamic loads is shown in Fig. 6, and the stress variation diagrams at points A and B are shown in Figs. 7 and 8. To obtain satisfactory results in the analysis, a mesh convergence study is required to select the optimal element size.

To generate an appropriate computational mesh, the sensitivity of the results from several meshes with different numbers of elements must be examined, and a mesh-independent solution must be achieved. The meshing of the intact blade and the blade with a V-shaped notch was analyzed using a 20-node cubic element and is shown in Fig. 3.

To investigate stress convergence, radial stresses were examined in the critical region of the intact blade and the blade with a V-shaped notch. Accordingly, a path was defined over the critical regions, and the analysis was repeated for different numbers of elements.

The radial stress results along the critical path in the intact blade are evaluated and plotted in Fig. 7 for different element counts. The graph indicates that the radial stress values have converged; therefore, 45,091 elements were used for all subsequent analyses of this blade.

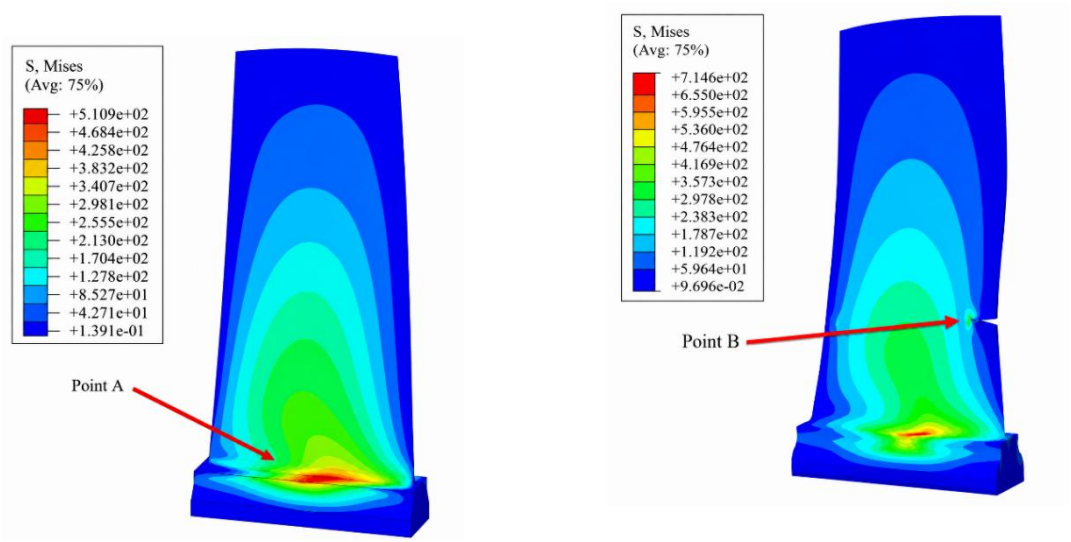


Fig. 6. Von Mises stress distribution in intact and with V-shaped notch compressor blades under combined centrifugal and aerodynamic loads.

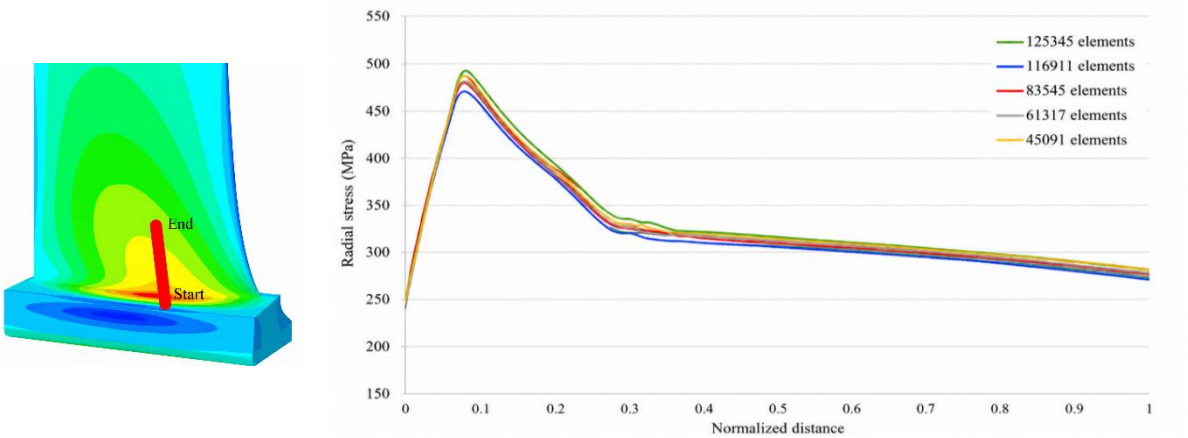


Fig. 7. Mesh independence study (radial stress distribution along the critical region of the intact blade).

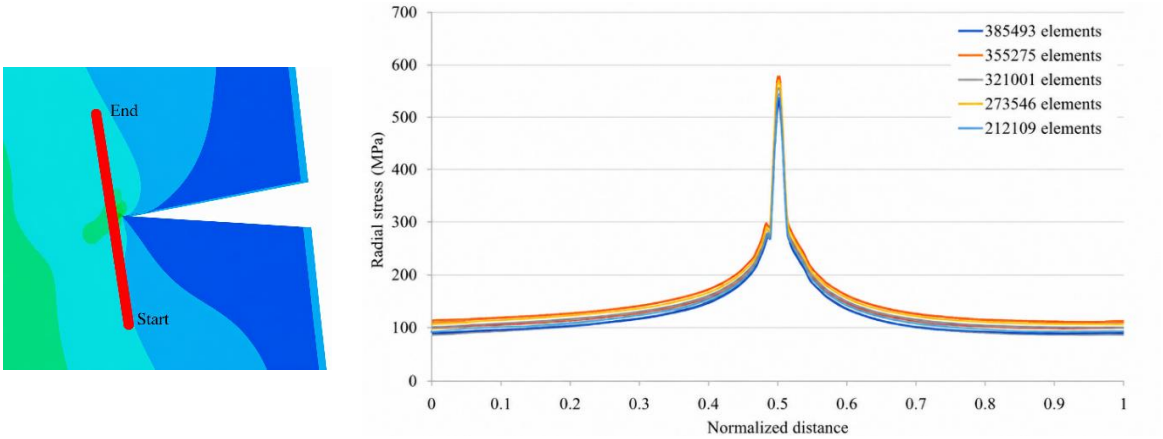


Fig. 8. Mesh independence study (radial stress distribution along the critical region of the blade with a V-shaped notch).

Furthermore, the radial stress results along the critical path in the blade with a V-shaped notch are evaluated in Fig. 8 for different element counts. As is evident in Fig. 8, the radial stress values have converged, and consequently, 212,109 elements were employed for all analyses of the blade with a V-shaped notch.

3. Assessment of critical areas of compressor blades

Based on the stress analysis of centrifugal loads and the stress analysis of aerodynamic loads, the stress distribution of the compressor blade was determined; hence, the areas of maximum stress, which are candidate locations for crack initiation and propagation, were identified and named as points A and B. In addition to the results of the stress analysis, there is abundant experimental evidence (Fig. 1) that proves points A and B correspond well to the failure area of the compressor blades in question.

Point A is the area of maximum stress of the intact blade at the root on the suction (convex) side of the blade (Fig. 6), and point B is the area of maximum stress in the blade with damage caused by a foreign object located in the V-shaped notch of the blade (Fig. 6), therefore, points A and B were selected for further evaluations of this research.

4. Prediction model, critical plane parameter determination, critical plane assessment, and fatigue life estimation

4.1. Fatigue life prediction model

For the fatigue life assessment of the first-stage compressor blade in a gas turbine, the Coffin–Manson theory [38] (Eq. (1)) is employed as the fundamental framework based on the Mises yield criterion (Eq. (2)) to predict the life.

$$\frac{\Delta\varepsilon_t}{2} = \frac{\sigma'_f}{E}(2N_f)^b + \varepsilon'_f(2N_f)^{b+c} \quad (1)$$

$$\Delta\varepsilon_t = \frac{\sqrt{2}}{3}\sqrt{(\varepsilon_1-\varepsilon_2)^2+(\varepsilon_2-\varepsilon_3)^2+(\varepsilon_1-\varepsilon_3)^2} \quad (2)$$

where $\Delta\varepsilon_t$ is the maximum principal strain amplitude, σ'_f and b are the fatigue strength coefficient and fatigue strength exponent, respectively, and ε'_f and c are the fatigue ductility coefficient and fatigue ductility exponent, respectively, and E is the elastic modulus, and N_f is the fatigue life.

The speed and working pressure of the compressor blade, as well as the effects of its own weight, create various stresses, such as tensile, compressive, and vibrational stresses. In addition, the Coffin-Manson equation is inapplicable in the presence of mean stresses, so the modified Morrow equation with mean stresses is used (Eq. (3)).

$$\frac{\Delta\varepsilon_t}{2} = \frac{\sigma'_f-\sigma_m}{E}(2N_f)^b + \varepsilon'_f(2N_f)^c \quad (3)$$

The Morrow equation is applicable for uniaxial loading and cannot be applied for multiaxial loading conditions for compressor blades. In the Smith-Watson-Topper (Eq. (4)) critical plane model [39], the normal and maximum stress ranges are calculated, and the critical plane with the maximum damage to the compressor blade is determined.

$$\sigma_{n,max}\frac{\Delta\varepsilon_{n,max}}{2}=\frac{(\sigma'_f)^2}{E}(2N_f)^{2b}+\sigma'_f\varepsilon'_f(2N_f)^{b+c} \quad (4)$$

where $\Delta\varepsilon_{n,max}$ is the maximum normal strain range and $\sigma_{n,max}$ is the maximum normal stress, on the plane with the maximum normal strain range.

Many experimental studies of multiaxial loadings have shown that normal strain ranges and shear strain ranges on the plane of maximum damage lead to multiaxial fatigue cracks.

The Smith–Watson–Topper model neglects the influence of shear strain and shear stress ranges on the critical plane, and the Brown-Miller model [40] (Eq. (5)) suggests that maximum fatigue damage occurs on the plane experiencing the maximum shear strain amplitude, which is a function of the normal strain and shear strain on this plane.

$$\frac{\Delta\gamma_{max}}{2}+\frac{\Delta\varepsilon_n}{2}=1.65\frac{\sigma'_f-\sigma_m}{E}(2N_f)^b+1.75\varepsilon'_f(2N_f)^c \quad (5)$$

where $\Delta\gamma_{max}$ is the maximum shear strain range and $\Delta\varepsilon_n/2$ is the normal stress range, on a plane with a maximum value of $(\Delta\gamma_{max}/2)+(\Delta\varepsilon_n/2)$.

Regarding the Brown-Miller model, the findings indicate that for complex loadings, the plane with the most damage is in better agreement with the plane with the largest value of $(\Delta\gamma_{max}/2)+(\Delta\varepsilon_n/2)$.

To investigate the effect of normal strain range and shear strain range, the Shang De-guang fatigue damage parameter [41] (Eq. (6)) is introduced, which is independent of the loading path and considers the maximum normal strain range and the maximum shear strain range on the plane with the maximum critical damage. The shear strain range $\Delta\gamma$ and the forward strain range ε_n^* between the two shear strain points are combined into a new equivalent strain amplitude that simultaneously considers the effect of the multiaxial loadings.

$$d=\frac{\Delta\varepsilon_{eq}}{2}=[\varepsilon_n^{*2}+\frac{1}{3}(\frac{\Delta\gamma_{max}}{2})^2]^{\frac{1}{2}} \quad (6)$$

Considering multiaxial loading conditions, a multiaxial fatigue life prediction model (Eq. (7)) for compressor blades is obtained, which is modified with the Morrow equation and combined with the Smith-Watson-Topper equation.

$$\sigma_{n,max}[\varepsilon_n^{*2}+\frac{1}{3}(\frac{\Delta\gamma_{max}}{2})^2]^{\frac{1}{2}}=\frac{(\sigma'_f)^2}{E}(2N)^{2b}+\sigma'_f\varepsilon'_f(2N)^{b+c} \quad (7)$$

It was subsequently observed that the shear stress, normal stress, and normal strain range on the maximum-failure critical plane influence multiaxial fatigue life, and consequently, the product of $\sigma_{n,max}$ and the equivalent strain amplitude is proposed as a novel fatigue damage parameter (Eqs. (8 and 9)).

$$d=\sigma_{n,max}[\varepsilon_n^{*2}+\frac{1}{3}(\frac{\Delta\gamma_{max}}{2})^2]^{\frac{1}{2}} \quad (8)$$

$$d=\frac{(\sigma'_f)^2}{E}(2N)^{2b}+(\sigma'_f)\varepsilon'_f(2N)^{b+c} \quad (9)$$

4.2. Determination of the critical plane parameter for multiaxial fatigue analysis of compressor blades

4.2.1. Algorithm for determining the critical plane

- From the finite element analysis of the compressor blade, the stress and strain tensors were evaluated throughout the loading history (Eq. (10)).
- The rotation tensor Q (Eqs. (11 and 12)) was determined by transferring the components from the diagonal plane of Fig. 8. The stress and strain tensors are transferred from the x, y, and z coordinates to the x′, y′, and z′ coordinates (Fig. 9) using the rotation tensor Q (Eqs. (13 and 14)).
- The plane determined at $\theta=0$ and $\varphi=0$ in the critical regions of the blade is taken as the first critical plane, and the stress and strain on the first critical plane are obtained under loading conditions [30].
- The plane determined at $\theta=0$ and $\varphi=0$ in the critical regions of the blade is taken as the first critical plane, and the stress and strain on the

first critical plane are obtained under loading conditions [30].

- The critical plane is the one that suffers the maximum damage; therefore, to determine it [41], the value of the damage parameter is determined in one-degree steps of θ and φ. To find the maximum damage parameter in terms of φ and θ, MATLAB software coding is applied. The angle between the normal strain projection in the x-y plane and the x-axis is called θ and its angle with the z-axis is called φ.

$$\sigma = \begin{pmatrix} \sigma_x & \tau_{xy} & \tau_{xz} \\ \tau_{yx} & \sigma_y & \tau_{yz} \\ \tau_{zx} & \tau_{zy} & \sigma_z \end{pmatrix} \qquad \varepsilon = \begin{pmatrix} \varepsilon_x & \varepsilon_{xy} & \varepsilon_{xz} \\ \varepsilon_{yx} & \varepsilon_y & \varepsilon_{yz} \\ \varepsilon_{zx} & \varepsilon_{zy} & \varepsilon_z \end{pmatrix} \tag{10}$$

$$\sigma' = Q^T \sigma Q \qquad \varepsilon' = Q^T \varepsilon Q \tag{11}$$

$$Q = \begin{pmatrix} a_{11} = \cos\theta\sin\varphi & a_{12} = \sin\theta\sin\varphi & a_{13} = \cos\varphi \\ a_{21} = -\sin\theta & a_{22} = \cos\theta & a_{23} = 0 \\ a_{31} = -\cos\theta\cos\varphi & a_{32} = -\sin\theta\cos\varphi & a_{33} = \sin\varphi \end{pmatrix} \tag{12}$$

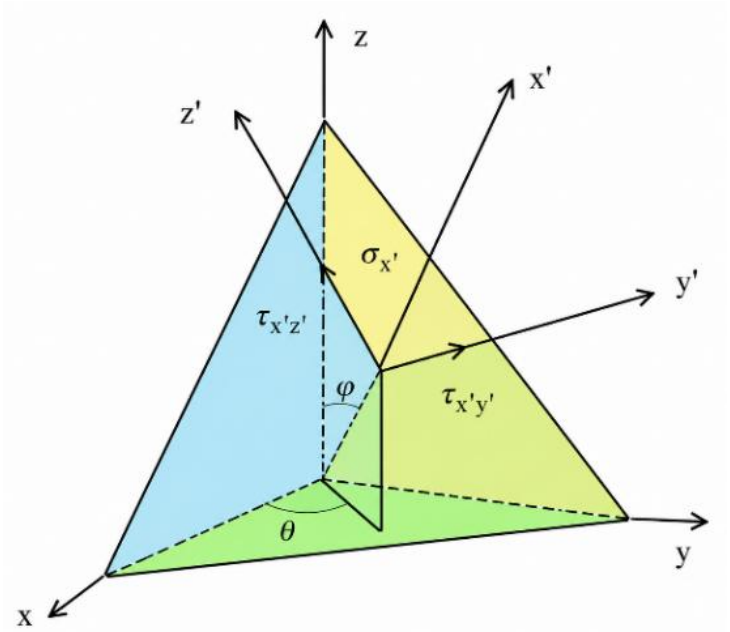


Fig. 9. Stress-strain on each plane.

$$\begin{pmatrix} \sigma_{x'} \\ \sigma_{y'} \\ \sigma_{z'} \\ \tau_{x'y'} \\ \tau_{y'z'} \\ \tau_{x'z'} \end{pmatrix} = \begin{pmatrix} a_{11}^2 & a_{12}^2 & a_{13}^2 & 2a_{11}a_{12} & 2a_{12}a_{13} & 2a_{11}a_{13} \\ a_{21}^2 & a_{22}^2 & a_{23}^2 & 2a_{21}a_{22} & 2a_{22}a_{23} & 2a_{21}a_{23} \\ a_{31}^2 & a_{32}^2 & a_{33}^2 & 2a_{31}a_{32} & 2a_{32}a_{33} & 2a_{31}a_{33} \\ a_{11}a_{21} & a_{12}a_{22} & a_{13}a_{23} & a_{12}a_{21}+a_{11}a_{22} & a_{13}a_{22}+a_{12}a_{23} & a_{13}a_{21}+a_{11}a_{23} \\ a_{21}a_{31} & a_{22}a_{32} & a_{23}a_{33} & a_{22}a_{31}+a_{21}a_{32} & a_{23}a_{32}+a_{22}a_{33} & a_{23}a_{31}+a_{21}a_{33} \\ a_{11}a_{31} & a_{12}a_{32} & a_{13}a_{33} & a_{12}a_{31}+a_{11}a_{32} & a_{13}a_{32}+a_{12}a_{33} & a_{13}a_{31}+a_{11}a_{33} \end{pmatrix} \begin{pmatrix} \sigma_x \\ \sigma_y \\ \sigma_z \\ \tau_{xy} \\ \tau_{yz} \\ \tau_{xz} \end{pmatrix} \tag{13}$$

$$\begin{pmatrix} \varepsilon_{x'} \\ \varepsilon_{y'} \\ \varepsilon_{z'} \\ \varepsilon_{x'y'} \\ \varepsilon_{y'z'} \\ \varepsilon_{x'z'} \end{pmatrix} = \begin{pmatrix} a^2_{11} & a^2_{12} & a^2_{13} & 2a_{11}a_{12} & 2a_{12}a_{13} & 2a_{11}a_{13} \\ a^2_{21} & a^2_{22} & a^2_{23} & 2a_{21}a_{22} & 2a_{22}a_{23} & 2a_{21}a_{23} \\ a^2_{31} & a^2_{32} & a^2_{33} & 2a_{31}a_{32} & 2a_{32}a_{33} & 2a_{31}a_{33} \\ a_{11}a_{21} & a_{12}a_{22} & a_{13}a_{23} & a_{12}a_{21}+a_{11}a_{22} & a_{13}a_{22}+a_{12}a_{23} & a_{13}a_{21}+a_{11}a_{23} \\ a_{21}a_{31} & a_{22}a_{32} & a_{23}a_{33} & a_{22}a_{31}+a_{21}a_{32} & a_{23}a_{32}+a_{22}a_{33} & a_{23}a_{31}+a_{21}a_{33} \\ a_{11}a_{31} & a_{12}a_{32} & a_{13}a_{33} & a_{12}a_{31}+a_{11}a_{32} & a_{13}a_{32}+a_{12}a_{33} & a_{13}a_{31}+a_{11}a_{33} \end{pmatrix} \begin{pmatrix} \varepsilon_x \\ \varepsilon_y \\ \varepsilon_z \\ \varepsilon_{xy} \\ \varepsilon_{yz} \\ \varepsilon_{xz} \end{pmatrix} \quad (14)$$

4.3. Assessment of critical planes based on different models

Based on the finite element results and experimental data obtained from monitoring the failure state of the compressor blades, candidate areas A and B were investigated. The stress and strain tensors of the assessment areas A and B are as shown in Table 4. In Fig. 10 and 11, the changes in the product of the maximum normal stress and the sum of the maximum shear strain amplitude and the forward strain range in terms of φ and θ (Shang De-Guang criterion) at points A and B are shown.

Additionally, the changes in the sum of the maximum shear strain amplitude and the normal strain amplitude in terms of φ and θ (Brown-Miller criterion) at points A and B are presented in the same figures, respectively [30, 41].

The maximum value of the shear strain amplitude was calculated through a degree-by-degree examination of the φ and θ angles over the loading history by coding in MATLAB software at points A and B, and the results are summarized in Table 5.

Furthermore, the maximum value of the sum of the maximum shear strain amplitude and the normal strain amplitude was listed in Table 5 following a degree-by-degree investigation of the φ and θ angles over the loading history via MATLAB coding at points A and B.

4.4. Fatigue life estimation

In this study, the life of the gas turbine compressor blade was estimated based on the Smith-Watson-Topper, Brown-Miller, and Shang De-Guang critical plane methods. Initially, the critical parameters of each of these criteria were determined separately. In the Smith-Watson-Topper criterion, the product of the maximum normal stress and the maximum normal strain amplitude was considered as the Smith-Watson-Topper parameter.

Table 4. Stress and strain components at assessment positions A and B.

Assessment position	Stress component (MPa)	Numerical value	Strain component (%)	Numerical value
A	σ_x	122.278	ε_x	-0.0137
	σ_y	136.427	ε_y	-0.0048
	σ_z	379.850	ε_z	0.1541
	τ_{xy}	3.434	ε_{xy}	0.0043
	τ_{yz}	-176.850	ε_{yz}	-0.2304
	τ_{xz}	8.322	ε_{xz}	0.0114
B	σ_x	212.719	ε_x	-0.0059
	σ_y	167.806	ε_y	-0.0349
	σ_z	606.689	ε_z	0.2481
	τ_{xy}	-0.358	ε_{xy}	-0.0004
	τ_{yz}	-40.935	ε_{yz}	-0.0528
	τ_{xz}	-289.193	ε_{xz}	-0.3730

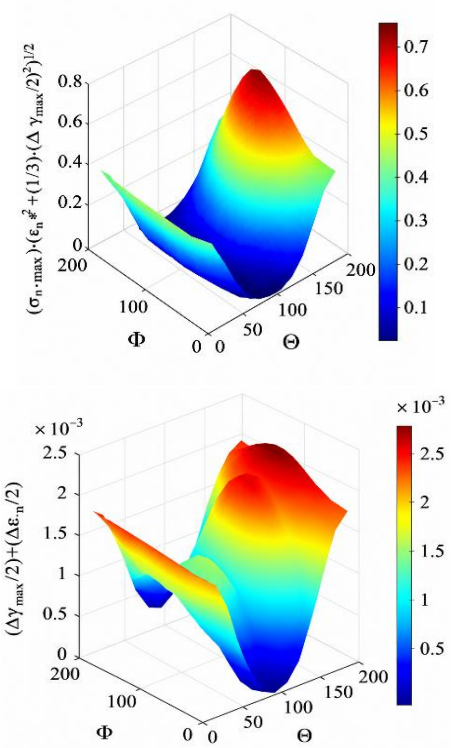


Fig. 10. Variation of the damage parameters of the Shang De-Guang criterion (upper graph) and the Brown–Miller criterion (lower graph) with respect to φ and θ at assessment point A.

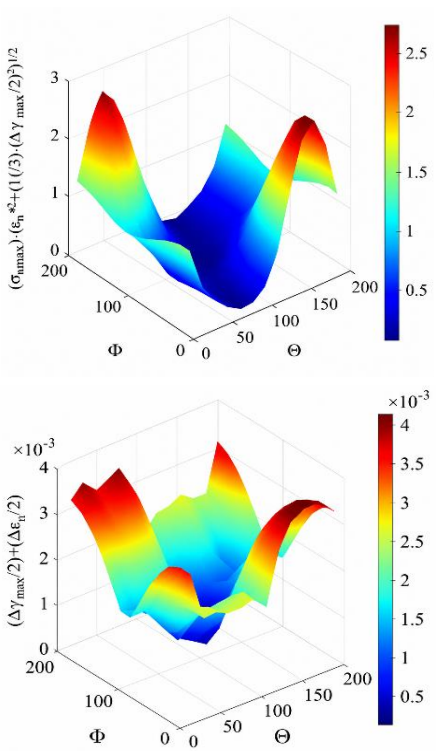


Fig. 11. Variation of the damage parameters of the Shang De-Guang criterion (upper graph) and the Brown–Miller criterion (lower graph) with respect to φ and θ at assessment point B.

In the Brown-Miller critical plane criterion, the product of the maximum shear strain amplitude and the normal strain amplitude was chosen as the Brown-Miller parameter, and in the Shang De-Guang criterion, the product of the maximum normal stress in a combination of the sum of the maximum shear strain amplitude and the forward strain range (Eq. (9)) is the effective parameter. The predicted lifetimes at the evaluated positions (derived from the aforementioned prediction methods) are presented in Table 6.

The data on the crack formation areas on the compressor blade indicate the importance of the low-cycle and high-cycle fatigue phenomena in the compressor blades. Therefore, in this study, the main focus was on investigating the fatigue behavior in the compressor blade. For this purpose, the candidate critical areas were initially determined by applying the finite element method.

The results of stress analysis and statistical data indicate that there is a good correspondence between the crack formation areas and stress concentration (Fig. 1).

According to the stress analysis results, the assessment areas A and B on the suction side (convex) in the intact blade fillet region and in the V-shaped notch of the blade with foreign object damage in Fig. 6 are close to the crack initiation area in Fig. 1, and they are consistent with the experimental data too.

Table 5. Results of searching for different critical planes at points A and B.

Assessment position	Fatigue model	θ (°)	φ (°)	d_{max}
A	Brown-Miller	155	93	0.0024
	Shang De-Guang	149	92	0.7773
B	Brown-Miller	143	5	0.0042
	Shang De-Guang	147	7	2.8562

Table 6. Results of life estimation of assessment positions A and B based on different methods.

Assessment position	Smith-Watson-Topper (cycles)	Brown-Miller (cycles)	Shang De-Guang (cycles)
A	8.61×10^8	2.14×10^9	7.16×10^8
B	3.86×10^5	8.70×10^5	3.20×10^5

Critical plane fatigue methods were applied to determine the crack propagation plane in the critical candidate areas. The critical planes determined based on the Brown-Miller and Shang De-Guang critical plane criteria for critical areas A and B are shown in Table 5 and Fig. 10 and 11.

Based on these criteria, the critical plane directions were determined in terms of φ and θ, and the calculated values are $143° < \theta < 155°$ and $2° < \varphi < 93°$. Due to the higher stress level of point B compared to point A, as expected, the life of point B is shorter than that of point A in all criteria.

The life prediction results indicate that the Brown-Miller method predicts a relatively longer life for points A and B, and the Shang De-Guang method provides the most conservative results. As expected from the results, given that the maximum stress at point B is greater than the fatigue strength of the compressor blade material, the blade life at point B was predicted to be finite, and at point A, given that the maximum stress is lower than the fatigue strength of the material, the blade life was predicted to be infinite, which can be clearly seen in Table 6.

For point A, the result of the Brown-Miller method is 2.37 times that of the Smith-Watson-Topper method and 2.86 times that of the Shang De-Guang method, and the result of the Smith-Watson-Topper method is 1.2 times that of the Shang De-Guang method.

Also, for point B, the result of the Brown-Miller method is 2.37 times that of the Smith-Watson-Topper method and 2.86 times that of the Shang De-Guang method, and the result of the Smith-Watson-Topper method is 1.2 times that of the Shang De-Guang method. Considering that compressor blades are designed for an infinite life, the predictions given for an intact blade with an infinite life seem reasonable. As is clear from the results in Table 6, the life of the defective blade due to foreign object damage is greatly reduced.

To further interpret the obtained results, the differences among the fatigue life predictions obtained from the applied critical plane criteria are discussed from an engineering perspective. The variations observed among the fatigue life estimations obtained from the Smith–Watson–Topper (SWT), Brown–Miller, and Shang De-Guang criteria are mainly associated with the different damage parameters and fatigue mechanisms considered by each model.

Although all three approaches are based on the critical plane concept, each criterion evaluates fatigue damage by assigning different importance to the normal stress, normal strain, and shear deformation components acting on the critical plane. Therefore, differences in predicted fatigue life are expected when these criteria are applied to components subjected to complex multiaxial loading conditions.

The SWT criterion evaluates fatigue damage based on the interaction between the maximum normal stress and normal strain amplitude. Accordingly, this criterion is strongly influenced by tensile loading effects and the mechanisms associated with crack opening during fatigue damage evolution. In compressor blades, centrifugal loading produces a considerable tensile stress component along the blade span direction; therefore, the SWT parameter can effectively capture the contribution of normal stress on fatigue behavior.

However, since the SWT criterion does not explicitly incorporate shear strain effects, its sensitivity may be reduced in regions where multiaxial stress states and significant shear deformation are generated due to local geometric discontinuities.

The Brown–Miller criterion considers the combined effect of shear strain amplitude and normal strain amplitude on the critical plane.

This approach is based on the assumption that fatigue damage under multiaxial loading is strongly influenced by cyclic shear deformation accompanied by normal strain effects. In the present study, the Brown–Miller criterion predicted the highest fatigue life values for both the intact and damaged blade conditions. This result indicates that, for the investigated loading condition, the damage parameter calculated by this criterion resulted in a lower fatigue damage estimation compared with the other approaches, and it led to less conservative fatigue life prediction.

In contrast, the Shang De-Guang criterion considers the combined influence of maximum normal stress, shear strain amplitude, and forward strain range in the fatigue damage parameter. By incorporating the interaction between normal and shear components, this

criterion provides a higher sensitivity to complex multiaxial stress and strain states.

This characteristic becomes particularly important for the blade containing foreign object damage, where the V-shaped notch introduces a severe local stress concentration and significantly modifies the stress–strain distribution near the critical region. Consequently, the Shang De-Guang criterion predicted the lowest fatigue life among the investigated methods, indicating a more conservative estimation of fatigue damage.

The differences among the fatigue life predictions are more pronounced for the damaged blade compared with the intact blade. For the intact blade, the stress state is primarily governed by centrifugal loading, and the absence of geometric discontinuities results in a relatively uniform stress distribution.

Consequently, all fatigue criteria predict a very high fatigue life, with relatively small differences among the obtained results. However, the presence of the V-shaped notch associated with foreign object damage generates a localized multiaxial stress concentration, increasing the complexity of the stress and strain fields around the notch root. Under such conditions, the ability of a fatigue criterion to account for the interaction between normal and shear components becomes more significant, resulting in larger differences among the predicted fatigue lives.

From an engineering perspective, the obtained results demonstrate that fatigue life prediction of compressor blades with foreign object damage is highly dependent on the selected critical plane fatigue model and its sensitivity to the local damage mechanism. Since FOD introduces a highly localized stress concentration and changes the multiaxial nature of the loading state, the selection of an appropriate fatigue criterion becomes particularly important for structural integrity assessment.

Conservative criteria may provide safer predictions for damage tolerance evaluations, whereas less conservative criteria may be useful for understanding fatigue behavior under specific loading conditions. Therefore, the application of multiple fatigue criteria provides a more comprehensive evaluation of the fatigue response and reduces the uncertainty associated with relying on a single fatigue life prediction approach.

It should be noted that the selection of an appropriate fatigue criterion should be performed considering the actual loading conditions, material characteristics, and available experimental evidence, since the predicted fatigue life can be influenced by the damage parameters and assumptions incorporated in each fatigue model.

Regarding the validation of the fatigue-life predictions, direct experimental fatigue data for the investigated blade configurations, including both the intact blade and the foreign-object-damaged blade, were not available; therefore, a direct one-to-one validation of the predicted fatigue lives was not possible. Nevertheless, the reliability of the adopted critical plane fatigue framework has been previously demonstrated through comparisons with experimental observations.

Huo *et al.* [41] evaluated the fatigue life of gas turbine blades using a critical plane approach and reported good agreement between numerical predictions and experimental results. Furthermore, in the authors' previous study [30], the Smith–Watson–Topper, Brown–Miller, and Shang De-Guang criteria were assessed, and the predicted fatigue lives were compared with the validated results reported in [41], confirming the applicability of these approaches for gas turbine blade fatigue assessment. Although the blade type and loading conditions differ from those considered in previous studies, the present analysis follows the same critical plane fatigue assessment framework and focuses on the comparative evaluation of intact and FOD-damaged blade configurations.

5. Conclusions

This study investigated the fatigue behavior of intact and foreign-object-damaged compressor blades using finite element stress analysis and critical-plane fatigue criteria. The finite element results indicated a strong correspondence between high-stress regions and experimentally observed crack initiation areas, confirming the capability of the numerical model to identify fatigue-critical zones.

Accordingly, two critical regions were selected for fatigue assessment: the fillet region on the suction side of the intact blade and the V-shaped notch induced by foreign object damage. The critical-plane analysis indicated that crack

propagation was strongly governed by the local multiaxial stress state, with predicted crack-plane orientations of approximately $143° < \theta < 155°$ and $2° < \varphi < 93°$.

The fatigue life assessment demonstrated that foreign object damage substantially reduced the fatigue resistance of the compressor blade. For the intact blade, the maximum stress remained below the fatigue strength, resulting in an infinite fatigue life prediction; however, the damaged blade exhibited finite fatigue life due to stress concentration at the V-shaped notch.

Among the applied criteria, the Brown–Miller method predicted the longest fatigue life, whereas the Shang De-Guang criterion provided the most conservative estimate and the Smith–Watson–Topper method gave intermediate results. The fatigue life predictions obtained by applying the Smith–Watson–Topper and Shang De-Guang methods were approximately 57.7% and 64.9% lower than those obtained by applying the Brown–Miller method, respectively.

References

[1] L. Witek, M. Wierzbińska and A. Poznańska, "Fracture analysis of compressor blade of a helicopter engine", *Eng. Fail. Anal.*, Vol. 16, No. 5, pp. 1616–1622, (2009).

[2] V. Troshchenko and A. Prokopenko, "Fatigue strength and life of compressor blades for marine gas turbine engines", *Strength Mater.*, Vol. 31, No. 1, pp. 18–27, (1999).

[3] A. Kermanpur, H. S. Amin, S. Ziaei-Rad, N. Nourbakhshnia and M. Mosaddeghfar, "Failure analysis of Ti6Al4V gas turbine compressor blades", *Eng. Fail. Anal.*, Vol. 15, No. 8, pp. 1052–1064, (2008).

[4] E. Silveira, G. Atxaga and A. Irisarri, "Failure analysis of a set of compressor blades", Eng. Fail. Anal., Vol. 15, No. 6, pp. 666–674, (2008).

[5] A. Poznanska, M. Sniezek and M. Wierzbinska, "Pitting corrosion–main factor generating fracture of the compressor of aeroengine blades under operation". Proc. of IX conf. "*Turbomachinery*", Rzeszow, pp. 439–46, (2003).

[6] E. Poursaeidi, A. Babaei, M. M. Arhani and M. Arablu, "Effects of natural frequencies on the failure of R1 compressor blades", *Eng. Fail. Anal.*, Vol. 25, pp. 304–315, (2012).

[7] A. Kolagar, N. Tabrizi, M. Cheraghzadeh and M. Shahriari, "Failure analysis of gas turbine first stage blade made of nickel-based superalloy", *Case Stud. Eng. Fail. Anal.*, Vol. 8, pp. 61–68, (2017).

[8] R. Mishra, V. Nandi and R. Raghavendra Bhat, "Failure analysis of high-pressure compressor blade in an aero gas turbine engine", *J. Fail. Anal. Prev.*, Vol. 18, No. 3, pp. 465–470, (2018).

[9] R. Mishra, J. Thomas, K. Srinivasan, V. Nandi and R. R. Bhatt, "Failure analysis of an un-cooled turbine blade in an aero gas turbine engine", *Eng. Fail. Anal.*, Vol. 79, pp. 836–844, (2017).

[10] A. Mokaberi, R. Derakhshandeh-Haghighi and Y. Abbaszadeh, "Fatigue fracture analysis of gas turbine compressor blades", *Eng. Fail. Anal.*, Vol. 58, pp. 1–7, (2015).

[11] A. Dadashi, E. Poursaeidi and S. Nasiri, "Stress concentration effect on the failure of an axial compressor first-stage rotating blades", *Mech. Based Des. Struct. Mach.*, Vol. 53, No. 5, pp. 3934–3956, (2024).

[12] T. Yokobori, H. Yamanouchi and S. Yamamoto, "Low cycle fatigue of thin-walled hollow cylindrical specimens of mild steel in uni-axial and torsional tests at constant strain amplitude", *Int. J. Fract. Mech.*, Vol. 1, No. 1, pp. 3–13, (1965).

[13] J. Morrow, "Cyclic plastic strain energy and fatigue of metals", *American Society of Testing and Materials*, STP. 43764S, pp. 45–87, (1965).

[14] D. Ji, M.-H. Shen, D. Wang and J. Ren, "Creep-fatigue life prediction and reliability analysis of P91 steel based on applied mechanical work density", *J. Mater. Eng. Perform.*, Vol. 24, No. 1, pp. 194–201, (2015).

[15] S. Suman, A. Kallmeyer and J. Smith, "Development of a multiaxial fatigue damage parameter and life prediction methodology for non-proportional loading", *Fract. Struct. Integr.*, Vol. 10, No. 38, pp. 224–230, (2016).

[16] F. Ellyin and B. Valaire, "High-strain multiaxial fatigue", *ASME J. Eng. Mater. Technol.*, Vol. 104, No. 3, pp. 165–173, (1982).

[17] Z.-R. Wu, X.-T. Hu and Y.-D. Song, "Multiaxial fatigue life prediction for titanium alloy TC4 under proportional and nonproportional loading", *Int. J. Fatigue*, Vol. 59, pp. 170–175, (2014).

[18] D. Kulawinski, M. Hoffmann, T. Lippmann, G. Lamprecht, A. Weidner, S. Henkel and H. Biermann, "Isothermal and thermo-mechanical fatigue behavior of 16Mo3 steel coated with high-velocity oxy-fuel sprayed nickel-base alloy under uniaxial as well as biaxial-planar loading", *J. Mater. Res.*, Vol. 32, No. 23, pp. 4411–4423, (2017).

[19] J. Mei and P. Dong, "A new path-dependent fatigue damage model for non-proportional multi-axial loading", *Int. J. Fatigue*, Vol. 90, pp. 210–221, (2016).

[20] N. R. Gates and A. Fatemi, "On the consideration of normal and shear stress interaction in multiaxial fatigue damage analysis", *Int. J. Fatigue*, Vol. 100, pp. 322–336, (2017).

[21] A. Ince and G. Glinka, "Innovative computational modeling of multiaxial fatigue analysis for notched components", *Int. J. Fatigue*, Vol. 82, 2, pp. 134–145, (2016).

[22] F. Öztürk, J. Correia, C. Rebelo, A. De Jesus and L. S. Da Silva, "Fatigue assessment of steel half-pipes bolted connections using local approaches", *Procedia Struct. Integr.*, Vol. 1, pp. 118–125, (2016).

[23] X.-F. Zhao, D.-G. Shang, Y.-J. Sun, M.-L. Song and X.-W. Wang, "Multiaxial fatigue life prediction based on short crack propagation model with equivalent strain parameter", *J. Mater. Eng. Perform.*, Vol. 27, No. 1, pp. 324–332, (2018).

[24] Z.-Y. Yu, S.-P. Zhu, Q. Liu and Y. Liu, "A new energy-critical plane damage parameter for multiaxial fatigue life prediction of turbine blades", *Mater.*, Vol. 10, No. 5, p. 513, (2017).

[25] Z. Lu, C. Chen, M. Qu, G. Li and H. Xuan, "Study on the Coupled Creep Fatigue Damage Characteristics of Single Crystal Blade Tenons Under High Speed Rotation and High Temperature Environments", *Fatigue Fract. Eng. Mater. Struct.*, Vol. 48, No. 12, pp. 5258–5272, (2025).

[26] Y. Xiao, H. Qin, K. Xu and Y. Wang, "Experimental study on fatigue-creep of P/M FGH96 superalloy with different holding time", *J. Northwest. Polytech. Univ.*, Vol. 38, No. 4, pp. 873–880, (2020).

[27] Z. Wang, W. Wu, J. Liang and X. Li, "Creep–fatigue interaction behavior of nickel-based single crystal superalloy at high temperature by in-situ SEM observation", *Int. J. Fatigue*, Vol. 141, p. 105879, 2020.

[28] X. Hu, Q. Zhang, Y. Jiang, G. Rao, G. Miao, W. He and X. Nie, "The effect of cyclic loading on the creep fatigue life and creep strength of a DS superalloy: Damage mechanism and life modeling", *Int. J. Fatigue*, Vol. 134, p. 105452, (2020).

[29] L. Sun, X. Zhang, R, Wang, X. Wang, S. Tu, K. Suzuki and H. Miura, "Evaluation of fatigue and creep-fatigue damage levels on the basis of engineering damage mechanics approach", *Int. J. Fatigue*, Vol. 166, p. 107277, (2023).

[30] A. Zolfaghari, A. R. Shahani and N. Asadpour, "Predicting the creep–fatigue life of a high-pressure gas turbine blade considering fluid–structure interaction", *Amirkabir J. Mech. Eng.*, Vol. 57, No. 8, pp. 1037–1068, (2025).

[31] L. Witek, "Numerical stress and crack initiation analysis of the compressor blades after foreign object damage subjected to high-cycle fatigue", *Eng. Fail. Anal.*, Vol. 18, No. 8, pp. 2111–2125, (2011).

[32] L. Li, B. Shang, B. Song and Y. Chen, "Analysis of Vibratory Stress and Crack

Growth of Compressor Blade Under HCF Loading", *J. Fail. Anal. Prev.*, Vol. 23, No. 04, pp. 1326–1343, (2023).
[33] W. Yin, Y. Liu, X. He, and Z. Tian, "High-Cycle Fatigue Strength Prediction Model for Ti-6Al-4V Titanium Alloy Compressor Blades Subjected to Foreign Object Damage", *Metals*, Vol. 15, No. 10, (2025).
[34] H. Moradi, R. Rafi and A. Muslim, "Crack growth simulation in 13th row of compressor blades under foreign object damage and resonant vibration condition", *J. Vibroeng.*, Vol. 23, No. 1, pp. 44–62, (2020).
[35] J. R. Davis, Stainless steels. ASM international, (1994).
[36] E. Poursaeidi, M. Arablu and M. Mohammadi Arhani, "Root cause analysis of unit 2 refinery powerplant gas turbine compressors 1st row rotating blade fractures", *south pars gas company*, Iran, (2010).
[37] E. Poursaeidi and H. Bakhtiari, "Fatigue crack growth simulation in a first stage of compressor blade", *Eng. Fail. Anal.*, Vol. 45, pp. 314–325, (2014).
[38] J. Tavernelli and L. Coffin, "Experimental support for generalized equation predicting low cycle fatigue", *J. Basic Eng.*, Vol. 84, No. 4, pp. 533–537, (1962).
[39] K. Smith, "A stress-strain function for the fatigue of metals", *J. Mater.*, Vol. 5, pp. 767–778, (1970).
[40] M. W. Brown and K. Miller, "A theory for fatigue failure under multiaxial stress-strain conditions", *Proc. Inst. Mech. Eng.*, Vol. 187, No. 1, pp. 745–755, (1973).
[41] J. Huo, D. Sun, H. Wu and W. Wang, "Multi-axis low-cycle creep/fatigue life prediction of high-pressure turbine blades based on a new critical plane damage parameter", *Eng. Fail. Anal.*, Vol. 106, p. 104159, (2019).

Copyrights ©2026 The author(s). This is an open access article distributed under the terms of the Creative Commons Attribution (CC BY 4.0), which permits unrestricted use, distribution, and reproduction in any medium, as long as the original authors and source are cited. No permission is required from the authors or the publishers.

How to cite this paper:

A. R. Shahani and A. Zolfaghari, "The estimation of the fatigue life of an intact gas turbine compressor blade and the same blade with foreign object damage based on critical plane methods", *J. Comput. Appl. Res. Mech. Eng.*, Vol. 15, No. 2, pp. 233-250, (2026).

DOI: 10.22061/jcarme.2026.113064.2825

URL: https://jcarme.sru.ac.ir/?_action=showPDF&article=12597